Protein-Water and Protein-Buffer Interactions in the Aqueous Solution of an Intrinsically Unstructured Plant Dehydrin: NMR Intensity and DSC Aspects

P. Tompa,* P. Bánki,† M. Bokor,† P. Kamasa,† D. Kovács,* G. Lasanda,† and K. Tompa†
*Institute of Enzymology, Biological Research Center, and †Research Institute for Solid State Physics and Optics, Hungarian Academy of Sciences, Budapest, Hungary

ABSTRACT Proton NMR intensity and differential scanning calorimetry measurements were carried out on an intrinsically unstructured late embryogenesis abundant protein, ERD10, the globular BSA, and various buffer solutions to characterize water and ion binding of proteins by this novel combination of experimental approaches. By quantifying the number of hydration water molecules, the results demonstrate the interaction between the protein and NaCl and between buffer and NaCl on a microscopic level. The findings overall provide direct evidence that the intrinsically unstructured ERD10 not only has a high hydration capacity but can also bind a large amount of charged solute ions. In accord, the dehydration stress function of this protein probably results from its simultaneous action of retaining water in the drying cells and preventing an adverse increase in ionic strength, thus countering deleterious effects such as protein denaturation.

INTRODUCTION

Protein function in general is manifested via a complex array of interactions between the protein and its molecular environment, most apparent in the case of interactions of the molecule with cofactors, ligands, and substrates, modifying enzymes, allosteric metabolites, targeting proteins, and other macromolecular binding partners. Underlying all these, however, is an intricate network of interactions with hydration water and solute ions that need to be replaced when the protein folds and interacts with its partners. Quantitative characterization of this latter, thus, is of prime importance for a molecular understanding of protein function.

A special aspect of protein hydration is the case of intrinsically unstructured proteins (IUPs), which do not fold into a well-defined three-dimensional (3D) structure under native, physiologic conditions (1–3). These proteins often realize their functions via molecular recognition, in which structural disorder confers specific advantages, such as specificity without excessive binding strength and many more. Because of their lack of a folded structure and largely exposed interaction surfaces, it is anticipated that the hydration of these proteins is significantly different from that of ordered, globular proteins. In fact, as reported in two recent articles, we used an NMR relaxation technique for characterizing the hydration of IUPs and found that their hydration is significantly higher than that of a globular control protein of similar size (4,5). Our observations provided a direct demonstration that IUP structure is more exposed than globular proteins and able to discriminate between fully and partially disordered classes of IUPs.

An interesting and thus far ill-characterized class of these proteins is late embryogenesis abundant (LEA) proteins. LEA proteins and one of their subclasses, dehydrins, provide protection to plants and free-living insects against deleterious consequences of water loss and freezing under dehydration stress conditions (6–8). The expression of these proteins is induced by osmotic stresses, such as draft, high salinity, and/or freezing, when they provide protection against hypoosmotic conditions. The mechanism of protection from the loss of water is unclear but could be by acting as hydration buffer, sequestering ions, protecting other proteins, renaturing unfolded proteins, or a combination of any of these (8,9). Probably all these functional aspects are underlined by their highly hydrophilic (10) and intrinsically unstructured nature, demonstrated for a handful of them thus far (11–15). The protein we characterize in this respect is the early responsive to dehydration (ERD) 10, expressed in plants in certain very actively dividing tissues and ubiquitously under drying conditions (16).

Our goal here is to gain information on water molecules in the solution of ERD10 and to characterize its structure by means of the separate study of the bound water fraction in aqueous solution by a combination of two different experimental methods. As far as bound water nomenclature is concerned, the terminology proposed by Cooke and Kuntz (17) is used: we refer to water molecules that are in the vicinity of and interact strongly with macromolecular surfaces and that have properties that are detectably different from those of the medium as ''bound water,'' and the remaining water as ''bulk water.'' By the term ''unfrozen water,'' we denote the actual fraction of water molecules in a mobile state at a given temperature. The unfrozen water term can therefore refer to a

Submitted March 8, 2006, and accepted for publication June 1, 2006.

Address reprint requests to P. Tompa, Institute of Enzymology, Biological Research Center, Hungarian Academy of Sciences, H-1518 Budapest, PO Box 7, Hungary. Tel.: 361-279-3143; Fax: 361-466-5465; E-mail: tompa@enzim.hu.

0006-3495/06/09/2243/07 $2.00

doi: 10.1529/biophysj.106.084723

phase composed of either bound water molecules only or bound plus bulk water molecules. We combine results from proton NMR intensity and differential scanning calorimetry (DSC) measurements on ERD10, a globular control (BSA), and buffer solution itself as reference to understand the special hydration/solvation properties of this IUP. Our results not only confirm that ERD10 has a high hydration potential but also provide the unexpected finding that this IUP has a large capacity and broad specificity for ion binding. The contribution of these factors to the function of this dehydration factor are discussed. In addition to these immediate implications, we also pursue this present line of research to develop experimental techniques, which provide quantitative structural and activity-related experimental data that characterize IUPs, as opposed to globular proteins.

EXPERIMENTAL

The applied NMR method is described in Bokor et al. (4) and Cooke and Kuntz (17). Shortly, the intensity of the NMR signal is measured as the amplitude of the free induction decay (FID) signal extrapolated to $t = 0$ and/or the Carr-Purcell-Meiboom-Gill (CPMG) echo train extrapolated to $t = 0$. Both quantities depend on the nuclear magnetization given by the standard formula as

$$M_0 \propto N_0 \frac{B_0}{T} \tag{1}$$

where B_0 is the static magnetic induction, N_0 is the number of contributing nuclei, and T is the absolute temperature. M_0 measures the number of protons (water molecules). The special aspects of NMR intensity measurements can be found in Tompa et al. (18). In the case of a multifraction system, both M_0 and N_0 represent the number of protons existing in a given phase, especially protons in a mobile state. The measurements were done on rapidly cooled and slowly reheated samples in the temperature range from -67 to $+30$°C. All the protons are in a mobile state (water molecules in liquid state) above 0°C, and we normalize the NMR intensities to this value accordingly.

In order to separate the various water phases present in aqueous solution samples (17), they were frozen. The phases of ice protons, organic protons, and bound water protons are clearly separated in the FID signal by virtue of large differences in the spin-spin relaxation rate (4). Ice protons yield a signal fraction characteristic of solids with a typical decay rate of the order of 10^5 s^{-1}. This signal is completely buried in the dead time of the spectrometer. Organic protons and/or irrotationally bound water protons (17) also yield a solid-like signal fraction with an order of magnitude smaller, but still large, decay rate. The proton NMR signal of unfrozen water has a much smaller time-domain decay rate, typically 2000 s^{-1}. This enables specific recording of the FID signal that belongs to bound water molecules. The zero-time extrapolated peak amplitude of the CPMG train gives the fraction of protons that belong to bound water molecules directly. The effect of freezing on the protein solutions was controlled by the comparison of NMR parameters obtained before and after a freeze-thaw cycle at temperatures above 0°C. We found that the freeze-thaw cycle caused no observable changes for the studied BSA and ERD10 solutions as far as the measured NMR parameters (FID amplitude, T1 and T2 relaxation times) are concerned.

The temperature was controlled by an open-cycle Oxford cryostat with an uncertainty better than ± 1 K. ^{1}H NMR measurements and data acquisition were accomplished by a Bruker SXP 4-100 NMR pulse spectrometer at frequencies of 44.1 and 82.6 MHz with a stability of better than $\pm 10^{-6}$. The data points in the figures are based on spectra recorded by averaging signals to reach a signal/noise ratio >50. We varied the number of averaged NMR signals to achieve the desired signal quantity for each sample and for unfrozen water quantities. We controlled the sensitivity of the NMR spectroscope by measuring the length of the $\pi/2$-pulse during measurements (18) to obtain reliable M_0 values. The extrapolation to zero time was done by fitting a stretched exponential.

Differential scanning calorimetry (DSC) measures the heat absorbed or emitted by the sample (enthalpy) subject to linearly scanned temperature. The temperature difference ΔT between reference and sample is strictly proportional to the heat capacity of the sample and to the heating rate:

$$\Delta T = \frac{mc_p}{K} q, \tag{2}$$

where m is the mass of the sample, c_p is its specific heat, q is the linear heating rate, and K is a constant defined by the construction of the DSC cell. The temperature difference ΔT is proportional to the heat flow we plotted (see Figs. 1, 3, and 4). The enthalpy change in the time interval t_1–t_2 can be obtained from the recorded temperature difference ΔT and is described by the following general formula:

$$\Delta H = K \int_{t_1}^{t_2} \Delta T \mathrm{d}t. \tag{3}$$

In a multifraction system such as our samples below 0°C, one can write similar terms for every fraction, namely for ice, for bound water, and for bulk or free water. The enthalpy change ΔH values (see Fig. 6) have an error of $\pm 5\%$.

The temperature is an intensive parameter of the system, so the relation between temperature and heat supplied to the sample describes its thermodynamic state. To obtain the true temperature of the sample in the calorimetric experiment, particularly for the case of phase transitions, the analysis of thermal paths among the sample, the temperature sensor, and the heat source is necessary. The DSC results presented here were temperature corrected using a procedure worked out during experiments with aqueous NaCl solutions. The details of temperature correction and enthalpy calculations are given elsewhere (19).

The DSC measurements were carried out at heating rate of $q = 2$ K min^{-1} on a TA Instruments heat-flux DSC. Before the experiment, the samples were cooled down with the same rate of $q = 2$ K min^{-1}. Cooling at an uncontrolled rate when the temperature changed exponentially from 15 K min^{-1} to a rate of less than 2 K min^{-1} at low temperatures had no observable influence on thermal behavior at heating. The NMR measurements were done at equilibrium state.

Sample

Double-distilled water was measured as a starting material to obtain calibration data and parameters for the temperature correction: 20 μl of liquid was used in DSC measurements and 100 μl in NMR. NaCl solution, 150 mM, was prepared by dissolving the appropriate quantity of NaCl (alt.) in distilled water. The Tris solution contained 50 mM Tris (Sigma, St. Louis, MO) and 1 mM EDTA (Sigma), pH 7.0. The buffer solution contained 150 mM NaCl, 50 mM Tris, and 1 mM EDTA, pH 7.0.

The aqueous protein solutions were prepared by dissolving the proper amounts of bovine serum albumin ((BSA); Sigma) or early responsive to dehydration 10 ((ERD10), prepared as described previously (4)) in the above buffer solution. For determining the amount of water bound per unit protein, and having noted that the concentration measurement of IUPs is error-prone because of their unusual reactions with colorimetric dyes, we directly measured the amount of protein dissolved by determining the mass of samples lyophilized from distilled water. This measure provided the absolute concentration of the protein, which could be directly used for calculating the absolute average concentration of its constituent amino acids. Given that NMR enabled the direct measurement of the concentration of bound water molecules, this allowed the calculation of the hydration of proteins normalized to amino-acid units, i.e., $n_{water}/n_{amino\ acid}$.

For each solution composition, we carried out the NMR and DSC measurements on three to five samples prepared independently. The obtained data were reproducible within the given statistical errors.

RESULTS AND DISCUSSION

We measured the thermal curves of pure water, NaCl solution, and buffer solution by DSC (Fig. 1). The heat capacity of ice determines the heat flow of water below 0°C. In this range, the specific heat of ice changes slightly from 1.703 J K^{-1} g^{-1} at −55°C to 2.07 J K^{-1} g^{-1} at +5.4°C (20). At 0°C, water exhibits a rapid increase of the heat flow that reflects the melting. At this point, the scale of the specific heat does not represent a real value. It is known that heat capacity at melting is extremely high. The heat flow returns exponentially to the level determined by the heat capacity of the liquid when melting is completed. This is a transient effect, which indicates how the sample temperature increases from the melting temperature to the stationary state of any transition. The heat capacity of the liquid (4.185 J K^{-1} g^{-1} at 22°C (21)) then determines the level of the heat flow on the curve of 150 mM NaCl solution. There are two marked differences, a small endothermic peak (SEP) at about −22°C and the continuous increase of heat flow up to 0°C. The Tris solution has a SEP at −13.6°C of much smaller amplitude and wider wings. The buffer solution shows a similar behavior with a small shift of the SEP toward lower temperatures than the NaCl solution of the same NaCl concentration.

We used double-distilled water as a control of NMR intensity measurements (Fig. 2 *a*). The unfrozen fraction changes from one to zero in the near vicinity of 0°C as expected. Traces of impurity cause a small deviation compared to a discrete jump from one to zero at exactly 0°C. The unfrozen water fraction in the NaCl solution (Fig. 2 *a*) shows

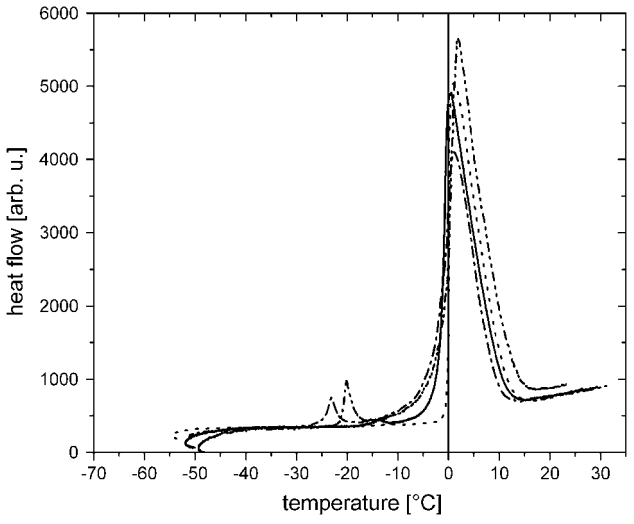

FIGURE 1 DSC curves measured in double-distilled water (*dotted line*), NaCl solution (*dash-dot-dotted line*), Tris solution (*solid line*), and buffer solution (*dash-dotted line*) in heating direction.

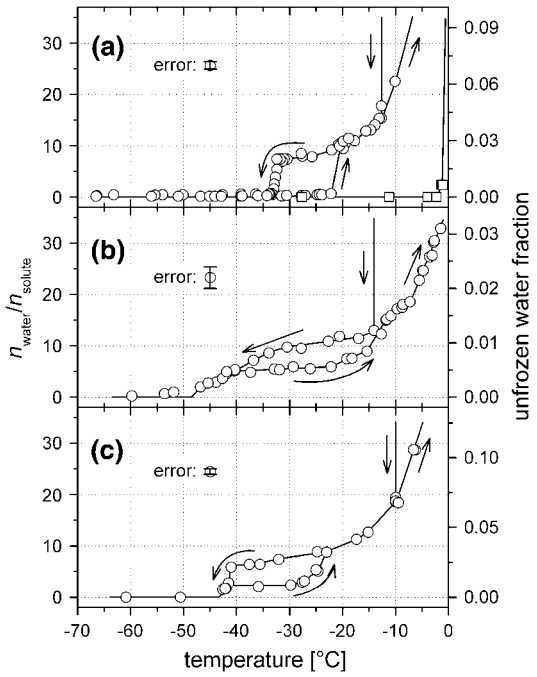

FIGURE 2 Mol fraction of unfrozen water molecules per solute unit (*left ordinate*) calculated from unfrozen water fraction measured by NMR signal intensity (*right ordinate*). (*a*) NaCl solution (*circles*); unfrozen fraction in distilled water (*squares*). (*b*) Tris solution. (*c*) Buffer solution. Lines are guides for the eye. Data points represent the means of five independent experiments ± SD (*error*).

characteristics absent in pure water because of the solute ions: a wide thermal hysteresis between −33°C and −22°C and then a smooth rise up to 0°C. The step in the unfrozen water fraction occurs at the same temperature in the heating direction as the SEP on the heat flow curve (also detected during heating). The smooth rise of the unfrozen water fraction above the hysteresis loop means that the melting starts at low temperatures and proceeds continuously up to 0°C. The Tris solution has a smaller unfrozen water fraction (Fig. 2 *b*) than the NaCl solution. The hysteresis loop extends to a wider temperature range between −40°C and −13°C and is quite shallow compared to that of NaCl. The curve of the buffer solution (Fig. 2 *c*) resembles more closely that of the NaCl solution, although its hysteresis loop gets wider and shifts to lower temperatures between −41°C and −25°C. In the case of both Tris and the buffer solution, the upper border of the hysteresis loop coincides with the corresponding SEP of the heating-mode DSC curve.

In the cointerpretation of these results, one can start from the NMR intensity data in pure water (Fig. 2 *a*). In the ice phase, there are no mobile water molecules at all: the zero-intensity range of the curve represents this state. We suppose that the small knee below 0°C is a consequence of the impurity hydration. In the NaCl, the Tris, and the buffer solution samples, the nonzero NMR intensity indicates the existence of unfrozen mobile water molecules. We calculated the number of unfrozen water molecules per solute

units (Fig. 2). In the NaCl solution (Fig. 2 *a*), the result of $n_{H_2O}/n_{NaCl} = 9.2 \pm 0.5$ at -22°C (upper side of the hysteresis loop) is in a quite reasonable agreement with 10 water molecules being in the first hydration shell of a water-mediated Na^+–Cl^- ion pair in liquid water as obtained by molecular dynamics simulations (22). And the value of $n_{H_2O}/n_{NaCl} = 7.4 \pm 0.5$ at -33°C (lower side of the hysteresis loop) agrees excellently with the quantity of seven water molecules in the first hydration shell of a close Na^+–Cl^- ion pair (without a water molecule between the two ions) in liquid water (22). Other authors calculated coordination numbers ranging from 10.68 to 18.33 for a NaCl unit (23). The n_{H_2O}/n_{NaCl} values obtained from our NMR intensity data fall within this interval in the temperature range determined by the freezing point in the cooling direction and the eutectic melting point in the heating direction. The comparison of the n_{water}/n_{solute} curves made between the buffer solution (Fig. 2 *c*) and its constituents (Fig. 2, *a* and *b*) reveals qualitative differences among the three solutions. The n_{water}/n_{solute} curve of the buffer solution cannot be reproduced as a weighted sum of the curves of its constituents.

An important inference from these observations is that buffer constituents (Tris and NaCl) are not independent in terms of hydration but interact with each other and partially replace water molecules that hydrate them. Further, the relatively large difference between the two sides of the hysteresis curves points to a significant change, and thus freedom of movement of hydration water around these solute ions. Our results demonstrate a novel experimental approach for the direct characterization of solute entities by measuring the number of water molecules that hydrate them at any temperature. The SEP and the sudden step in the unfrozen water fraction (NMR intensity) on heating are both attributed to the change in the motional state of hydration H_2O molecules, most presumably in the first hydration shell. The great endothermic peak is the DSC response to the solid-liquid first-order phase transformation. The low-temperature shift and the widening of the hysteresis loop in the buffer solution are consequences of the interaction of solute molecules Tris, EDTA, and NaCl, as the NaCl concentrations are the same in the NaCl solution and in the buffer solution.

The DSC and unfrozen water fraction (NMR intensity) data obtained for aqueous solutions of the proteins BSA ($c_{protein} = 50$ mg/cm^3, Fig. 3) and ERD10 ($c_{protein} = 25$ mg/cm^3, Fig. 4) are in striking contrast to the results for the NaCl, the Tris or the buffer solutions (Figs. 1 and 2). The quantity of bound (unfrozen) mobile water and the heat flow change continuously below 0°C as expected. The real surprise is the absence of hysteresis in the mobile water fraction and the lack of the SEP in the protein solutions! The bound water fraction for the BSA solution has a gentle slope below -25°C with values of 0.040 ± 0.002 at -25.5°C and 0.020 ± 0.002 at -53.5°C. The water content of BSA solution freezes completely between -53.5 and -55.6°C. In

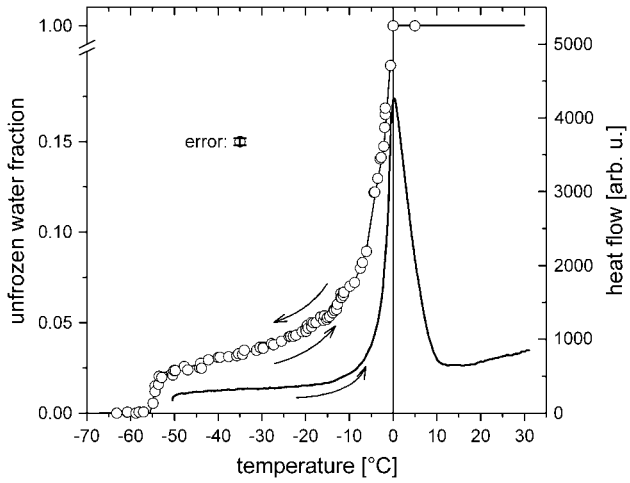

FIGURE 3 DSC curve (*line*) and unfrozen water fraction (*circles*) in 50 mg/cm^3 BSA solution. Data points represent the means of five independent experiments ± SD (*error*).

contrast to the BSA solution, the bound water fraction for the ERD10 solution changes significantly even below -25°C. It is diminishing steadily from the value of 0.055 ± 0.002 at -25.5°C to the value of 0.024 ± 0.002 at -46.7°C. The remaining mobile water fraction freezes completely at around -48°C, at a much higher temperature than in the case of the BSA solution.

To make a quantitative comparison between the two proteins, the number of mobile water molecules per amino acid unit ($n_{water}/n_{amino\ acid}$) was calculated for the concentration-normalized number of amino acids (see Experimental), which provides a direct and comparable measure of the hydration capacity of the two proteins. The results are plotted against temperature in Fig. 5. We decided on the norm to be the amino acid unit to obtain a parameter independent of the actual length or amino acid composition of the particular

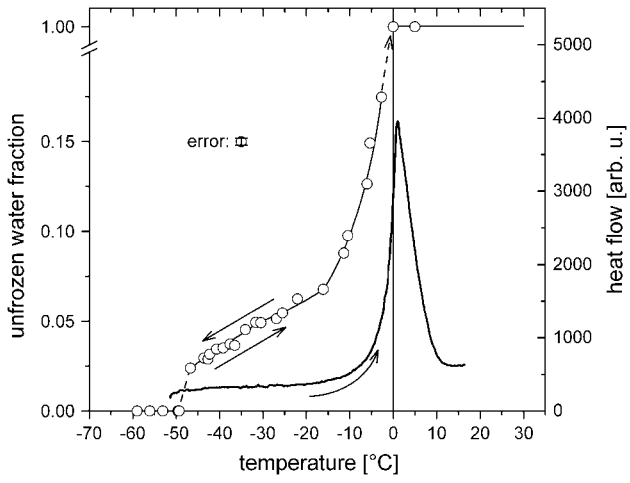

FIGURE 4 DSC curve (*line*) and unfrozen water fraction (*circles*) in 25 mg/cm^3 ERD10 solution. Data points represent the means of five independent experiments ± SD (error).

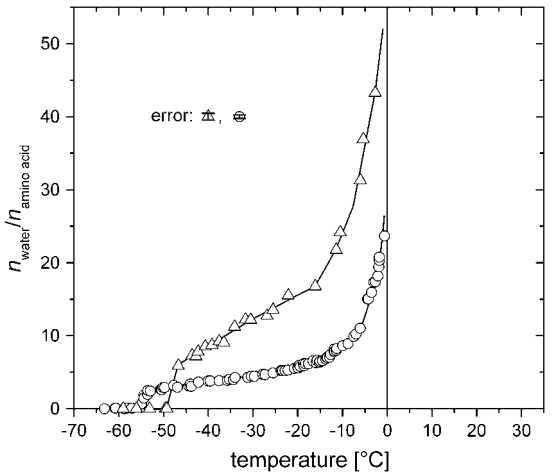

FIGURE 5 Number of unfrozen water molecules per amino acid unit in 50 mg/cm^3 BSA solution (*circles*) and in 25 mg/cm^3 ERD10 solution (*triangles*). Lines are guides for the eye. Data points represent the means of five independent experiments ± SD (*error*).

protein and of the protein concentration of the solution. The hydration (bound unfrozen water fraction) differs markedly for the globular protein BSA and the IUP ERD10. The $n_{water}/n_{amino\ acid}$ parameter has a value of 4.9 ± 0.2 at −25.5°C for the BSA solution, and it reaches its lowest value of 2.5 ± 0.2 at −53.5°C. We measured $n_{water}/n_{amino\ acid} = 5.9 \pm 0.5$ for the ERD10 solution just before complete freezing, which is 2.4 times greater. The value 13.5 ± 0.5 for the ERD10 solution at −25.5°C is 2.8 times higher than it is for the BSA solution. These quite large differences between the IUP and the globular protein reflect a much larger binding capacity for water of the IUP molecule. In principle, such a difference is expected from previous two-dimensional (2D) electrophoresis studies (24), which have placed ERD10 among IUPs. The novel 2D technique, however, only provides a qualitative assessment of the gross structural status of the proteins, whereas the approach presented here enables a quantitative estimation of the exposure of the polypeptide chain manifest in its hydration. In effect, this higher hydration is quantitative evidence for the unstructured nature of this protein. Our previous comparison of two IUPs (calpastatin and MAP2c) (5) has shown that quantification of hydration permits a deeper insight into the structure of IUPs, which segregate into structural subclasses of different levels of disorder, such as random coil, molten globule, and premolten globule (25). Taken at face value, the data calculated here suggest that ERD10 is practically fully disordered, best approximated by the random coil state.

In theory, these measured values could also be interpreted in terms of the average solvent accessible surface area (SASA) of ERD10. This would provide information on what portion of SASA is actually accessible to water, or how effectively residues in contact with water modify water structure and result in hydration resistant to freezing alongside bulk water molecules. Because of the inherent structural heterogeneity of an IUP, however, there is no independent estimate of SASA other than measuring its hydration directly, as carried out here. Thus, at present one cannot tell if this or any other IUP binds more or less water than expected for a globular protein of similar SASA. As discussed below, the hydration of the IUP and the globular BSA do show qualitative differences in terms of heterogeneity, which can be seen from the slope of unfrozen water fraction versus temperature curves and the ultimate freezing point, which may point to their principally different mechanisms of water binding. Further studies, however, will be needed to elucidate these points.

Although these differences among proteins of different structural status were expected in light of prior data (4,5), the contrasting behavior of the protein solution and its buffer is very surprising. A reasonable question is what quantity of protein molecules are necessary to cancel the thermal hysteresis of the unfrozen water fraction and the SEP. To address this issue, we studied a series of protein solutions by changing the protein concentration only. The integral areas of SEPs plotted in Fig. 6 are proportional to the enthalpy change of the eutectic phase separation (Eq. 3). The integral area of the SEP decreases and the hysteresis fades away as the protein concentration is increased for both types of proteins. The most striking difference between the two protein types lies in the minimal protein concentration necessary to suppress the SEP or the hysteresis: it is between 8 and 12.5 mg/cm^3 for ERD10, whereas there is a big SEP even at a BSA concentration of 25 mg/cm^3. These results prove the more pronounced water-binding activity of the IUP ERD10 than of the globular protein BSA.

These results, however, also point to an unexpected aspect of protein action in that the absence of the hysteresis/SEP

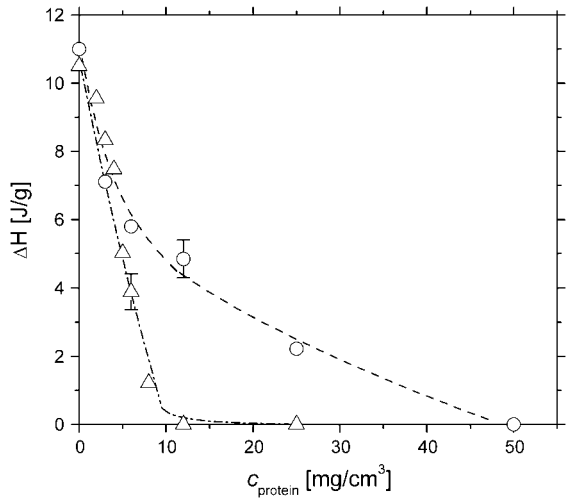

FIGURE 6 Integral area of the small endothermic peak of the DSC curve as a function of protein concentration for BSA (*circles*) and ERD10 solutions (*triangles*). Lines are guides for the eye. Data points represent the mean of five independent experiments ± SD (*error*).

from the curves suggests that independent hydration of solute ions is very effectively abolished by ERD10. This suggests that the hydration layer of Tris/NaCl is replaced by the protein, which ''solvates'' the ions. This finding fits nicely with prior suggestions on the molecular mechanisms of how LEA proteins counter the damage caused by dehydration/freezing conditions. These proteins may offer various ways for maintaining homeostasis under such conditions, such as membrane protection, chaperone action, water retention and ion sequestration (8,9). None of these putative mechanisms has received unequivocal and general experimental verification thus far. Our results presented here, and in a previous paper (4), demonstrate the high hydration capacity of this and probably other LEA proteins. Further, hydration of this protein and that of BSA show significant differences, in the sense that hydration of the IUP ERD10 is rather heterogeneous, with an array of distinct binding sites. The steady and steep increase in the amount of unfrozen water on heating can be interpreted as melting of ice phases at different temperatures. The melting of different ice phases can be interpreted as a change in the motional state (dynamics) of water molecules bound at different binding sites. BSA, on the other hand, behaves very differently in that it contains fewer and more homogeneous binding sites, the hydration water of which freezes at a temperature 7°C lower. The lowest mobile water concentration of 2.5 ± 0.2 water molecules per amino acid of the BSA solution equals the threshold level of hydration (0.40 g of water per gram of protein) required to fully activate the dynamics and functionality of globular proteins (26–28).

Large-scale binding of solute ions to the protein is a novel finding that deserves further consideration. Shrinking of cytosol volume as a result of water loss is detrimental to cells for several reasons, one being protein denaturation and salting-out, which occur because of an increase in ionic strength. For this reason, the cell's defense strategy is to produce small organic osmolytes (sugars) for maintaining osmotic equilibrium and lowering ion concentration by sequestering ions. This latter may be yet another function of largely disordered LEA proteins, underscored by the evidence presented here that ERD10 binds a large number of ions. A similar but more specific capacity has been shown for its homolog ERD14 (29) and has been suggested as a rather general function of IUPs acting as ''metal sponges'' (1). This effect, in combination with the high hydration capacity of IUPs and their noted chaperone activity (30), may explain the general observation that high-level expression of ''hydrophilins'' (10) is a general and evolutionarily conserved response to a variety of dehydration stress conditions, such as draft, salinity, and freezing.

Conclusions and outlook

The main results of our work can be summarized as follows:

- We propose a novel method for quantitative measurement of water molecules in the hydration shell directly based on NMR intensity data for NaCl and protein-buffer aqueous solutions.
- The thermal hysteresis in the NMR intensity curve of the NaCl–water solution is connected with changes in the motional state of protons belonging to hydration-shell water molecules, probably the start of rotational motion of these water molecules.
- The DSC-versus-temperature curve consists of contributions from changes in the motional state of water molecules, heat capacities of the constituent phases, and the heat of melting, where appropriate.
- A small endothermic peak was detected in the DSC curves at the same temperature range where the thermal hysteresis exists in the NMR intensity curves. The ordinary explanation of bordering steps of the NMR-intensity hysteresis loop is to assume activation and deactivation of rotational molecular motion of hydration water molecules at the appropriate temperatures. The rotational motion is probably the initial step of the eutectic phase separation (the literary interpretation of thermal properties of salt solutions (brines) (31,32)).
- Tris and EDTA additives to NaCl solution cause shifts in NMR-intensity hysteresis and temperature of the small endothermic peak. These qualitative changes refer to interaction of NaCl with the small molecular constituents.
- Both the thermal hysteresis in the NMR intensity curve and the SEP disappeared in the protein-buffer solution at a given protein concentration. The limits and character of disappearance are markedly different for the selected globular protein and IUP.
- The thermal behavior and the value of NMR intensities themselves are also characteristically different for the two types of proteins, which reveals the differences in the quantity and the kinetic behaviors of hydration shell water molecules.

Open questions are the following:

- Do the same effects exist in the cases of other proteins? How far can the above-summarized results be generalized? It is of immediate note that cooling and freezing applied in the present experiments may affect the protein's native conformation. Reversibility does hold, as repeated NMR experiments done before and after the freeze–thaw cycle leave the NMR parameters unaffected. A major conformational change can also be ruled out, as the reported parameters (FID intensity and DSC response) do not depend on the speed of cooling. Further experiments with extremely fast cooling will be required to control and rule out finer structural effects.
- What is the role of the other members of the buffer in the processes that result in the disappearance of the NMR-intensity hysteresis and the SEP?
- NMR measurements on ^{23}Na and ^{35}Cl nuclei can give direct proof of bound water molecules in the immediate neighborhood of ions or of interacting ion–protein units.

We intend to look for other physical methods offering similar responses to these questions.

This work was supported by the International Senior Research Fellowship GR067595 from the Wellcome Trust. Peter Tompa acknowledges the support of the Bolyai János Scholarship.

REFERENCES

1. Dunker, A. K., C. J. Brown, J. D. Lawson, L. M. Iakoucheva, and Z. Obradovic. 2002. Intrinsic disorder and protein function. *Biochemistry.* 41:6573–6582.
2. Tompa, P. 2002. Intrinsically unstructured proteins. *Trends Biochem. Sci.* 27:527–533.
3. Dyson, H. J., and P. E. Wright. 2005. Intrinsically unstructured proteins and their functions. *Nat. Rev. Mol. Cell Biol.* 6:197–208.
4. Bokor, M., V. Csizmok, D. Kovacs, P. Banki, P. Friedrich, P. Tompa, and K. Tompa. 2005. NMR relaxation studies on the hydrate layer of intrinsically unstructured proteins. *Biophys. J.* 88:2030–2037.
5. Csizmok, V., M. Bokor, P. Banki, É. Klement, K. F. Medzihradszky, P. Friedrich, K. Tompa, and P. Tompa. 2005. Primary contact sites in intrinsically unstructured proteins: the case of calpastatin and microtubule-associated protein 2. *Biochemistry.* 44:3955–3964.
6. Ingram, J., and D. Bartels. 1996. The molecular basis of dehydration tolerance in plants. *Annu. Rev. Plant Physiol. Plant Mol. Biol.* 47:377–403.
7. Thomashow, M. F. 1999. Plant cold acclimation: freezing tolerance genes and regulatory mechanisms. *Annu. Rev. Plant Physiol. Plant Mol. Biol.* 50:571–599.
8. Wise, M. J., and A. Tunnacliffe. 2004. POPP the question: what do LEA proteins do? *Trends Plant Sci.* 9:13–17.
9. Bray, E. A. 1993. Molecular responses to water deficit. *Plant Physiol.* 103:1035–1040.
10. Garay-Arroyo, A., J. M. Colmenero-Flores, A. Garciarrubio, and A. A. Covarrubias. 2000. Highly hydrophilic proteins in prokaryotes and eukaryotes are common during conditions of water deficit. *J. Biol. Chem.* 275:5668–5674.
11. Eom, J., W. R. Baker, A. Kintanar, and E. S. Wurtele. 1996. The embryo-specific EMB-1 protein of Daucus carota is flexible and unstructured in solution. *Plant Sci.* 115:17–24.
12. Lisse, T., D. Bartels, H. R. Kalbitzer, and R. Jaenicke. 1996. The recombinant dehydrin-like desiccation stress protein from the resurrection plant *Craterostigma plantagineum* displays no defined three-dimensional structure in its native state. *Biol. Chem.* 377:555–561.
13. Soulages, J. L., K. Kim, C. Walters, and J. C. Cushman. 2002. Temperature-induced extended helix/random coil transitions in a group 1 late embryogenesis-abundant protein from soybean. *Plant Physiol.* 128:822–832.
14. Goyal, K., L. Tisi, A. Basran, J. Browne, A. Burnell, J. Zurdo, and A. Tunnacliffe. 2003. Transition from natively unfolded to folded state induced by desiccation in an anhydrobiotic nematode protein. *J. Biol. Chem.* 278:12977–12984.
15. Koag, M. C., R. D. Fenton, S. Wilkens, and T. J. Close. 2003. The binding of maize DHN1 to lipid vesicles. Gain of structure and lipid specificity. *Plant Physiol.* 131:309–316.
16. Kiyosue, T., K. Yamaguchi-Shinozaki, and K. Shinozaki. 1994. Characterization of two cDNAs (ERD10 and ERD14) corresponding to genes that respond rapidly to dehydration stress in *Arabidopsis thaliana*. *Plant Cell Physiol.* 35:225–231.
17. Cooke, R., and I. D. Kuntz. 1974. The properties of water in biological systems. *Annu. Rev. Biophys. Bioeng.* 3:95–126.
18. Tompa, K., P. Bánki, M. Bokor, G. Lasanda, and J. Vasáros. Diffusible and residual hydrogen in amorphous Ni(Cu)-Zr-H alloys. 2003. *Journal of Alloys and Compounds.* 350:52–55.
19. Kamasa, P., M. Bokor, M. Pyda, and K. Tompa. 2006. Temperature correction for heat capacity and phase transformation studies of water solutions in heat-flux-type calorimeters. *Thermochimica Acta.* In press.
20. Giauque, W. F., and J. W. Stout. 1936. The entropy of water and the third law of thermodynamics. The heat capacity of ice from 15 to 273 K. *J. Am. Chem. Soc.* 58:1144–1150.
21. Jessel, A. R. C. S. 1934. The effect of dissolved air on the specific heat of water. *Proc Phys Soc.* 46:747–763.
22. Khalack, J. M., and A. P. Lyubartsev. 2004. Car-Parinello molecular dynamics simulations of Na^{+}-Cl^{-} ion pair in liquid water. *Condens. Matter Phys.* 7:683–698.
23. Zhou, J., X. Lu, Y. Wang, and J. Shi. 2002. Molecular dynamics study on ionic hydration. *Fluid Phase Equilib.* 194–197:257–270.
24. Csizmok, V., E. Szollosi, P. Friedrich, and P. Tompa. 2006. A novel two-dimensional electrophoresis technique for the identification of intrinsically unstructured proteins. *Mol. Cell. Proteomics.* 5:265–273.
25. Uversky, V. N. 2002. Natively unfolded proteins: a point where biology waits for physics. *Protein Sci.* 11:739–756.
26. Kuntz, I. D., Jr., and W. Kauzmann. 1974. Hydration of proteins and polypeptides. *Adv. Protein Chem.* 28:239–345.
27. Rupley, J. A., and G. Careri. 1991. Protein hydration and function. *Adv. Protein Chem.* 41:37–172.
28. Poole, P. L., and J. L. Finney. 1983. Sequential hydration of a dry globular protein. *Biopolymers.* 22:255–260.
29. Alsheikh, M. K., B. J. Heyen, and S. K. Randall. 2003. Ion binding properties of the dehydrin ERD14 are dependent upon phosphorylation. *J. Biol. Chem.* 278:40882–40889.
30. Tompa, P., and P. Csermely. 2004. The role of structural disorder in the function of RNA and protein chaperones. *FASEB J.* 18:1169–1175.
31. Koop, T., A. Kapilashrami, L. T. Molina, and M. J. Molina. 2000. Phase transitions of sea-salt/water mixtures at low temperatures: implications for ozone chemistry in the polar marine boundary layer. *J. Geophys. Res.* 105:26393–26402.
32. Cho, H., P. B. Shepson, L. A. Barrie, J. P. Cowin, and R. Zaveri. 2002. NMR investigation of the quasi-brine layer in ice/brine mixtures. *J. Phys. Chem. B.* 106:11226–11232.